Journal of Pharmaceutical and Biomedical Analysis 54 (2011) 789–798

Contents lists available at ScienceDirect

Journal of Pharmaceutical and Biomedical Analysis

journal homepage: www.elsevier.com/locate/jpba

Metabolic profiling of GuanXin II prescription based on metabolic fingerprinting and chemical analysis

Xue Qiao, Jian Han, Man Xu, Zi-chuan Zhang, Min Ye*, Guan Ye, De-an Guo*

The State Key Laboratory of Natural and Biomimetic Drugs, School of Pharmaceutical Sciences, Peking University, 38 Xueyuan Road, Beijing 100191, China

ARTICLE INFO

Article history:
Received 8 August 2010
Received in revised form
26 September 2010
Accepted 21 October 2010
Available online 29 October 2010

Keywords:
GuanXin II prescription
Formulated Chinese medicine
LC/MS
Metabolic profile

ABSTRACT

A sensitive LC/MS method was established to investigate the in vivo metabolism of GuanXin II prescription, a five-component Chinese herbal medicine formulation. Rat plasma, bile, urine, and feces were collected and analyzed following oral administration of the water decoction. A total of 50 compounds were identified, including 17 prototypes and 33 metabolites underwent methylation, oxidation, hydrolysis, sulfate conjugation, glucuronide conjugation, and glutathion conjugation. In addition, the component herb of the formulation from which the metabolites were derived was also identified. Among the five component herbs, Rhizoma Chuanxiong, Flos Carthami, and Lignum Dalbergiae Odoriferae were actively metabolized, contributing 26 metabolites and 2 prototypes, while Radix Salviae Miltiorrhizae and Radix Paeoniae Rubra underwent less biotransformation, yielding 7 metatbolites and 15 prototypes. This is the first study on the metabolic profile of GuanXin II prescription. The results could be valuable to elucidate the material basis of this formulated Chinese medicine.

1. Introduction

GuanXin II prescription (GX II, Guan-Xin-Er-Hao in Chinese) is a formulated Chinese medicine. It has been used to treat coronary artery diseases in China for decades. Clinical studies revealed it could improve blood circulation, protect cardiac muscle cells, and regulate hemodynamic ischemia modified albumin [1,2].

GX II is composed of five herbs in the ratio of 2:1:1:1:1. Among them, Radix Salviae Miltiorrhizae accounts for the largest proportion and plays the major therapeutic role together with Rhizoma Chuanxiong. They act as the emperor herb according to the Traditional Chinese Medicine formulation theory. Radix Paeoniae Rubra and Flos Carthami play the auxiliary role (or minister herb), and Lignum Dalbergiae Odoriferae plays the assisting role (or assistant and messenger herb). Up to date, more than 200 compounds, mainly phenolic acids, hydrophobic tanshinones, phthalides, alkaloids, monoterpene glycosides, flavonoids and volatile oils [3–9], have been reported from these herbs.

Pharmacokinetic studies of the major chemical constituents of GX II, such as salvianolic acid B [10], paeoniflorin [11], ligustilide [12], butylidenephthalide [13] and hydroxysafflor yellow A [14], have been widely reported. Besides, metabolic fingerprinting has been used to investigate the metabolism of component herbs [15]. However, no report is available to profile the in vivo metabolites of GX II prescription due to its complicated chemical composition.

In recent years, developments in analytical techniques allow intensive study on the metabolites of complex herbal preparations. Particularly, liquid chromatography coupled with tandem mass spectrometry (LC/MS/MS) could be used for targeted metabolic screening which identified metabolites, as well as for non-targeted metabonomic studies which led to the discovery of biomarkers [16–20]. However, these methods were based on adequate understanding of either the targeted metabolites or specific endogenous compounds affected by the medication.

Metabolite profiling provides important evidences to elucidate the mechanism of herbal medicines [21]. Liquid chromatography coupled with mass spectrometry (LC/MS), given its efficient chromatographic separation, high detection sensitivity, and strong structural elucidation capabilities, has been one of the most powerful techniques for herbal metabolite identification [21–24]. However, to the best of our knowledge, few studies have been conducted to profile the in vivo metabolites of formulated TCM prescriptions by using LC/MS.

In the present study, LC/MS was used to analyze biological samples (rat plasma, bile, urine, and feces) collected after oral administration of GX II decoction. A total of 50 compounds were identified or tentatively assigned, including 17 prototypes and 33 metabolites. Furthermore, the in vivo metabolic pathway of GX II was proposed. This was the first metabolic study on GuanXin II pre-

Abbreviations: LC/MS, liquid chromatography coupled with mass spectrometry; GSH, glutathione; GX II, GuanXin II prescription(Guan-Xin-Er-Hao in Chinese); RDA cleavage, retro-Diels-Alder cleavage; TCM, traditional Chinese medicine; TIC, total ion current.

* Corresponding authors. Tel.: +86 10 82801516; fax: +86 10 82802700.
E-mail addresses: yemin@bjmu.edu.cn (M. Ye), gda5958@163.com (D.-a. Guo).

0731-7085/$ – see front matter © 2010 Elsevier B.V. All rights reserved.
doi:10.1016/j.jpba.2010.10.017

scription, in which the metabolic pathways of its major compounds were elucidated through LC/MS metabolic fingerprints.

2. Experimental

2.1. Chemicals and materials

All reference standards were isolated and purified in our laboratory [3]. Purities of the standards were above 98% by HPLC analysis. Acetonitrile (Caledon, Canada) and de-ionized water (prepared by a Milli-Q Water purification system, Millipore, MA, USA) were of HPLC grade. Methanol, acetic acid and other chemicals were of analytical grade. High-purity nitrogen (99.99%) and helium (99.999%) were purchased from Gas Supplies Center of Peking University Health Science Center (Beijing, China).

Radix Salviae Miltiorrhizae, Rhizoma Chuanxiong, Radix Paeoniae Rubra and Flos Carthami were purchased from TianHeng Pharmacy (Beijing, China), Lignum Dalbergiae Odoriferae was purchased from China Crude Drug Co. Ltd. All the herbal materials were authenticated by Prof. De-an Guo. GX II decoction and the individual herbs were separately extracted according to our previously reported protocol [9], and then freeze-dried to obtain samples (in loose powder) for animal studies.

2.2. Animals and drug administration

Sprague–Dawley rats (male, 12–14 weeks; 200–240 g) were provided by the Experimental Animal Center, Peking University Health Science Center, China. Protocols of animal experiments were approved. Animals were kept in an environmentally controlled breeding room for 3 days and fasted 12 h before experiments. GX II freeze-dried powder was dissolved in 9 g/L NaCl solution (NS) (500 mg/ml) and administered by oral gavage at a dose of 3000 mg/kg (equivalent to 15 g of crude drug per kg) body weight to medication group I. Freeze-dried powder of the single herbs was dissolved to 500 mg/ml in NS solution, and administered orally at 600 mg/kg body weight to medication group II. Equivalent NS solution was given to the blank group.

2.3. Sample collection and pretreatment

After the oral administration of GX II, blood samples were collected at 15, 30, 50 and 100 min ($n = 5$), centrifuged (9000 rpm) for 10 min, and the supernatant was separated. Bile, urine and feces samples were collected over 0–12 h, 12–24 h and 24–36 h periods ($n = 3$). All samples were stored at −80 °C until analysis.

For plasma and urine samples, Oasis® HLB SPE columns (pre-eluted with 6 ml of methanol and 6 ml of de-ionized water) were used for pretreatment. Samples (2 ml) were washed with 6 ml of de-ionized water and then eluted with 6 ml of methanol–water (4:1, v/v), successively. For bile samples, 2 ml of bile was mixed with 300 μl of 10% (v/v) hydrochloric acid, vortex for 2 min, mix with 6 ml of ethyl acetate, vortex again for 5 min, centrifuge (9000 rpm) for 5 min, and the supernatant was transferred to a clean test tube. For feces samples, 2 g of dried samples were extracted with 12 ml of methanol–water (4:1, v/v) in an ultrasonic bath for 30 min, and centrifuged (9000 rpm) for 5 min. The supernatant was transferred to a clean test tube. The above solutions were evaporated to dryness under a gentle flow of nitrogen at 35 °C, and reconstituted in 200 μl of methanol. All samples were filtered through a membrane (0.22 μm pore size), and a 10 μl aliquot was injected into LC/MS.

2.4. LC/MS conditions

The LC/MS system consisted of an Agilent 1100 series HPLC instrument (a quaternary pump, a diode-array detector, an autosampler and a column compartment; Agilent, Waldbronn, Germany) coupled to a Finnigan LCQ Advantage ion trap mass spectrometry (Thermo Finnigan, San Jose, CA, USA) through an ESI interface. All data were processed by Xcalibur™ 1.3 (Thermo Finnigan, San Jose, CA).

Samples were separated on a Zorbax Extend-C_{18} reversed-phase column (5 μm, 250 mm × 4.6 mm, Agilent) protected with a Zorbax Extend-C_{18} guard column (5 μm, 12.5 mm × 4.6 mm, Agilent). The mobile phase consisted of acetonitrile (A) and water containing 0.3% (v/v) formic acid (B). Gradient program: 0–5 min, 2% A; 5–10 min, 2%–10% A; 10–55 min, 10%–26% A; 55–75 min, 26%–50% A; 75–80 min, 50%–90% A, 80–90 min, 90% A. Flow rate, 1.0 ml/min. Column temperature, 25 °C. For MS detection, ultra-high purity helium (He) was used as the collision gas and high purity nitrogen (N_2) as the nebulizing gas. The source-dependent parameters were optimized for different structural types (Table 1S). Scan range, *m/z* 100–1000; isolation width, 4.0 Th.

3. Results and discussion

3.1. Optimization of LC/MS conditions

To obtain the optimal settings for spray voltage, capillary temperature, capillary voltage and tube lens offset voltage, five reference compounds were selected and injected continuously (0.1–0.2 mg/ml in methanol) into the ESI source. The optimized settings (Table 1S) were applied to the analyses of component herbs.

3.2. Identification of metabolites

Metabolites identification was based on: (1) maximum UV absorption, (2) known compounds previously reported from GX II, (3) MS and MS^n ($n = 2$–4) spectra, and (4) MS^n fragmentation patterns of the metabolites.

The metabolic pathways of GX II constituents were remarkably different and highly dependent on chemical structures [25]. Therefore, the metabolites were categorized according to their structural types in the following discussion. Major constituents of GuanXin II and their metabolites are shown in Fig. 1. In total, 50 peaks were assigned as GX II metabolites in various bio-samples, including 18 phenolic acids, 22 flavonoids, 4 pinanes, and 6 phthalides (Table 1).

3.2.1. Phenolic acids

A total of 11 prototypes and 7 metabolites derived from phenolic acids were identified. They were mostly detected in bile and feces, except 2 hydrophilic metabolites found in urine.

Among the 11 prototypes, peaks **1**, **6**, **29** and **34** were identified by comparing with reference standards. Peaks **26**, **35**, **38** and **39** produced fragment ions in high accordance with the study of Liu et al. [3], and were identified as dimeric and trimeric phenolic acids. Peaks **41**, **42** and **44** (Fig. 2A) showed similar retention time and same $[M-H]^-$ ion at *m/z* 731. The MS/MS, MS^3 and MS^4 spectra yielded prominent ions at *m/z* 533, 335 and 320 by the loss of danshensu, another danshensu and methyl, respectively, which indicated a methyl group connected to furan ring. Therefore, peak **42** were assigned as 4-*O*-methyl salvianolic acid B [3], peaks **41** and **44** were proposed as 3′ or 4′-*O*-methyl salvianolic acid B in accordance with previous study [26].

In terms of metabolites, peak **17** was proposed as hydroxyl-salvianolic E, which showed a similar fragmentation pathway to salvianolic E (*m/z* 717) [3,25]. Its $[M-H]^-$ ion at *m/z* 735 suggested hydration (18 u) or the substitution of a hydroxyl group (16 u) combined with hydrogenation. Peak **20** was proposed as dimer of the known salvianolic acid D [3]. Peaks **47**, **48** (Fig. 2B) and **49** were methylated derivatives of salvianolic B [27]. Peak **33** exhibited an additional 80 u in its $[M-H]^-$ ion at *m/z* 797 (Fig. 1B1), which

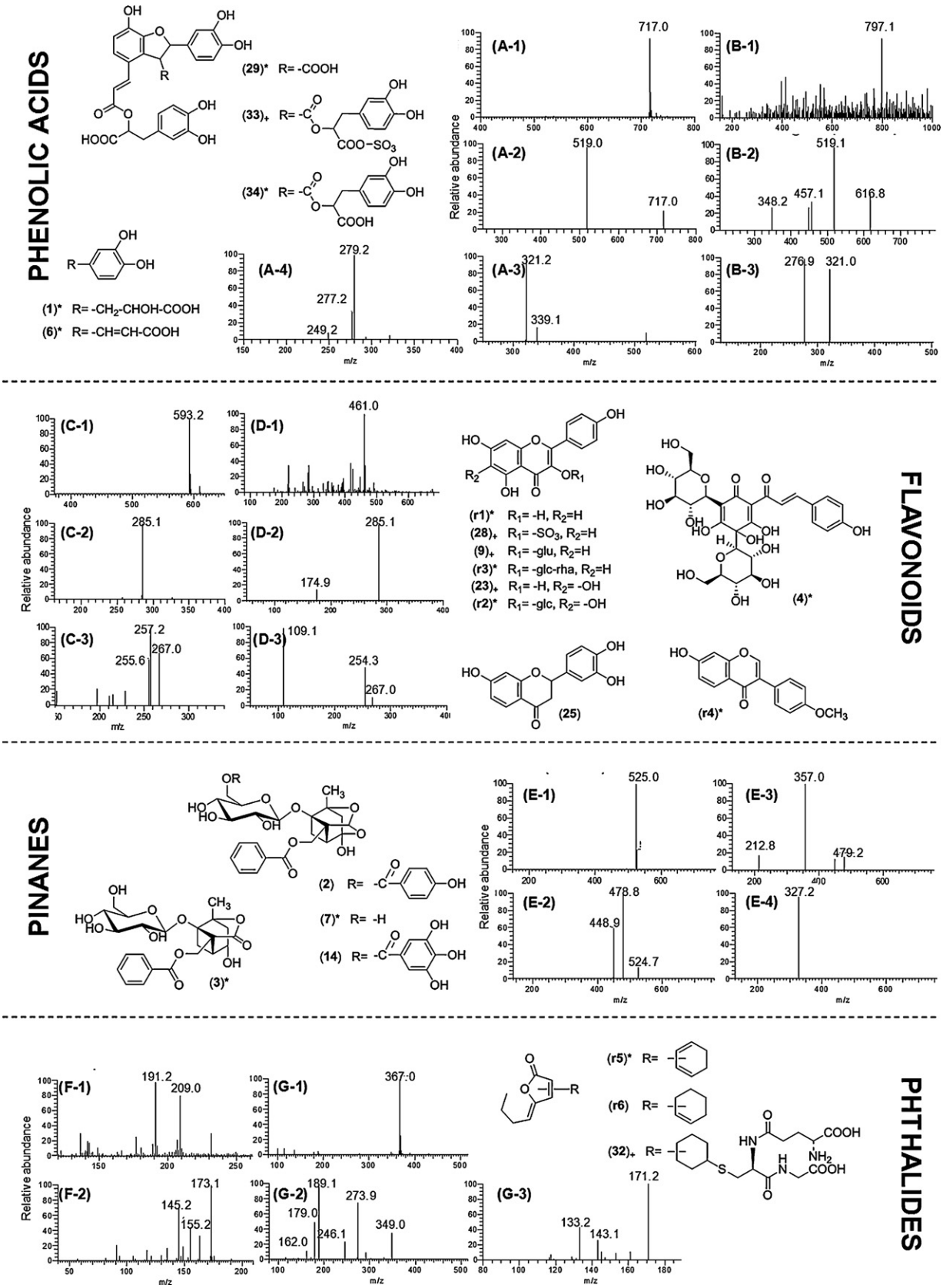

Fig. 1. Major chemical components of GuanXin II prescription and selected metabolites identified by LC/MS. *Note for spectra*: (A)–(F) salvianolic acid B (**34**), salvianolic acid B sulfate (**33**), kaempferol-3-*O*-β-rutinoside (**r3**), kaempferol glucuronide (**9**), paeoniflorin (**7**), ligustilide (**r6**), and ligustilide glutathione conjugate (**32**); 1–4: MS full scan, MS/MS, MS^3, and MS^4 spectra. *Note for schemes*: numeric ID with brackets, compounds identified in rat biological samples following the administration of GX II; "**r**" + numeric ID with brackets, compounds detected in GX II decoction only, referring to previous studies (see Table 2S and [9]); *compared with reference compounds; + identified as metabolites.

Table 1
Identification of GuanXin II prescription metabolites in SD rats after oral administration.

No.	Retention time, t_R (min)	$[M-H]^-$ (m/z)	$[M+H]^+$ (m/z)	Assigned identification	HPLC/ESI-MS^n m/z (% of relative abundance)	Type of metabolism[b]		Detected in[c]				Origin[d]	Ref.[e]
								P	B	U	F		
Phenolic acids													
1	12.17	197		Danshensu[a]	MS^2[197]: 179(100)	–	N/A	–	+	–	+	D	
5	18.76	178		Benzoyl glycine	MS^2[178]: 135(49), 134(100)	I	X	–	+	+	–	D	[27]
6	19.66	179		Caffeic acid[a]	MS^2[179]	–	N/A	–	–	+	–	D	
17	37.81	735		Hydroxylsalvianolic E	MS^2[735]: 537(100), 519(19), 493(8), 357(6), 321(10), 297(8), 295(6) MS^3[735–537]: 519(37), 475(12), 449(12), 357(74), 339(30), 321(100), 297(69), 295(88), 253(13)	I	O	–	+	–	+	D	[3,25]
20	40.62	835		Salvianolic acid D	MS^2[835]: 640(24), 417(100)	I	X	–	+	–	–	D	[3]
26	43.20	717		Salvianolic acid E	MS^2[717]: 519(100), 321(22) MS^3[717 → 519]: 339(28), 321(100) MS^4[717 → 519 → 321]: 303(7), 292(6), 279(100), 277(60), 268(8)	–	N/A	–	–	–	+	D	[3]
29	46.03	493		Lithospermic acid[a]	MS^2[493]: 313(11), 295(100) MS^3[493 → 295]: 295(7), 281(9), 280(14), 277(43), 276(6), 267(22), 266(6), 251(15), 250(18), 185(15), 175(21), 159(69), 109(100)	–	N/A	–	–	–	+	D	
33	49.73	797		Salvianolic acid B sulfate	MS^2[797]: 673(7), 634(6), 519(100), 321(36) MS^3[797 → 519]: 321(95), 277(100)	II	S	–		–	+	D	[3,25]
34	50.06	717		Salvianolic acid B[a]	MS^2[717]: 519(100), 321(26) MS^3[717 → 519]: 339(21), 321(100) MS^4[717 → 519 → 321]: 293(12), 279(100), 277(33), 249(8)	–	N/A	–	+	–	+	D	
35	50.82	717		iso-Salvianolic acid B	MS^2[717]: 519(100), 321(15) MS^3[717 → 519]: 339(15), 321(100), 279(9) MS^4[717 → 519 → 321]: 283(17), 279(100), 277(73), 249(17)	–	N/A	–	–	–	+	D	[3]
38	53.67	717		Salvianolic acid L	MS^2[717]: 519(100), 321(22) MS^3[717 → 519]: 339(21), 321(100), 279(6) MS^4[717 → 519 → 321]: 303(6), 293(22), 279(100), 277(55), 249(8)	–	N/A	–	–	–	+	D	[3]
39	54.27	493		Salvianolic acid A	MS^2[493]: 413(7), 317(100)	–	N/A	–	+	–	+	D	[3]
41	56.38	731		3′or 4′-*O*-Methyl salvianolic acid B	MS^2[731]: 533(100), 335(11) MS^3[731 → 533]: 353(35), 335(100), 320(8) MS^4[731 → 533 → 335]: 320(100), 319(6), 291(8)	–	N/A	–	+	–	+	D	[3]
42	57.15	731		4-*O*-Methyl salvianolic acid B	MS^2[731]: 533(100), 353(6), 335(13) MS^3[731 → 533]: 353(38), 335(100), 320(7), 309(6) MS^4[731 → 533 → 335]: 320(100), 307(6), 276(7)	–	N/A	–	+	–	+	D	[3]
44	58.63	731		3′or 4′-*O*-Methyl salvianolic acid B	MS^2[731]: 533(100), 335(9) MS^3[731 → 533]: 353(28), 335(100), 320(11) MS^4[731 → 533 → 335]: 320(100), 278(44), 276(14)	–	N/A	–	+	–	+	D	[3]
47	61.12	745		3′,3‴-*O*-Dimethyl-salvianolic acid B	MS^2[745]: 533(100), 353(6), 335(16) MS^3[745 → 533]: 353(40), 335(100), 320(6) MS^4[745 → 533 → 335]: 320(100), 307(6), 292(6), 291(10)	II	M	–	+	–	–	D	[26]
48	62.79	745		3′,3″-*O*-Dimethyl-salvianolic acid B	MS^2[745]: 547(100), 533(10), 353(7), 335(16) MS^3[745 → 547]: 353(38), 335(100), 320(13) MS^4[745 → 547 → 335]: 320(100), 307(7), 292(6), 291(11), 263(9)	II	M	–	+	–	–	D	[26]
49	65.18	759		3′,3″,3‴-*O*-Trimethyl-salvianolic acid B	MS^2[759]: 547(100), 353(9), 335(15) MS^3[759 → 547]: 353(50), 335(100), 320(8) MS^4[759 → 547 → 335]: 320(100), 306(13), 302(9)	II	M	–	+	–	–	D	[26]

Flavonoids												
4	17.61	611	Hydroxysafflor yellow A[a]	MS^2[611]: 491(100), 473(15), 403(25), 325(17) MS^3[611 → 491]: 473(100), 455(10), 427(6), 353(9), 323(18), 301(14), 283(35), MS^4[611 → 491 → 473]: 456(100), 429(22), 413(32), 353(48), 323(58), 247(54), 233(36), 231(64)	–	N/A	+	–	+	+	H	
8	26.78	555	3′-Hydroxymelanttin glucuronide	MS^2[555]: 475(77), 379(100) MS^3[555 → 379]: 299(100) MS^4[555 → 379 → 299]: 284(100)	II	G	+	–	–	–	J	[8,25]
9	28.51	461	Kaempferol glucuronide	MS^2[461]: 285(100), 175(7) MS^3[461 → 285]: 267(18), 255(57), 109(100)	I, II	H, G	+	–	+	–	H	[7,25]
10	32.28	431	Isoliquiritigenin glucuronide	MS^2[431]: 387(17), 255(100), 175(32)	II	G	+	–	–	–	J	[28]
11	32.43	527	Butein glucuronide sulfate	MS^2[527]: 447(11), 351(100) MS^3[527 → 351]: 271(100) MS^4[527 → 351 → 271]: 177(61), 151(100), 119(53)	II	G, S	+	–	–	–	J	[8,25]
13	33.35	431	Liquiritigenin glucuronide	MS^2[431]:297(5), 255(100), 175(60) MS^3[255]:135(100),153(32) MS^4[153]:135(100)	II	G	+	–	–	–	J	[28]
18	37.97	395	Violanone sulfate	MS^2[395]: 315(100) MS^3[395 → 315]: 300(100), 285(15), 191(10) MS^4[395 → 315 → 300]: 285(94), 269(100), 224(19), 192(6), 191(9), 178(6), 176(7), 135(30)	II	S	+	–	–	–	J	[8,25]
19	40.14	461	Vestitone glucuronide	MS^2[461]: 443(18), 399(15), 285(100), 175(16) MS^3[461 → 285]: 267(23), 257(100), 239(23), 149(76), 121(45)	I, II	H, G	–	+	+	–	J	[8,25]
22	40.91	491	Violanone glucuronide	MS^2[491]: 315(100), 174(9), 157(9) MS^2[491]: 371(68), 315(34), 177(28), 175(100)	II	G	–	+	–	–	J	[8,25]
23	41.20	381	6-Hydroxykaempferol sulfate	MS^2[381]: 301(100) MS^3[381 → 301]: 283(81), 254(100)	II	S	+	–	+	–	H	[7,25]
24	41.28	447	Butein glucuronide	MS^2[447]: 271(100), 175(36) MS^3[447 → 271]: 177(19), 169(9), 151(100), 93(19)	II	G	–	+	+	–	J	[8,25]
25	41.53	271	Butin	MS^2[271]: 227(10), 211(6), 151(100), 119(7)	–	N/A	–	–	–	+	J	[8]
28	45.69	365	Kaempferol sulfate	MS^2[365]: 285(100) MS^3[365 → 285]: 109(100)	I, II	H, S	+	–	+	–	H	[7,25]
30	46.67	477	(3*R*)-4′-Methoxy-2′,3,7-trihydroxyisoflavanone glucuronide	MS^2[477]: 301(100), 175(10) MS^3[477 → 301]: 286(17), 283(100), 258(14), 257(46), 242(50) MS^4[477 → 301 → 283]: 225(100)	II	G	+	+	–	–	J	[8,25]
31	47.02	439	Methyl-5,7-dihydroxy-trimethoxyisoflavanone sulfate	MS^2[439]: 359(100) MS^3[439 → 359]: 344(100), 329(13) MS^4[439 → 359 → 344]: 329(100), 328(23), 315(23), 314(15), 311(21), 301(64), 270(45), 233(24)	I, II	M, S	–	+	+	–	J	[8,25]
36	51.42	491	5,7-Dihydroxy-2′,4′-dimethoxyisoflavanone glucuronide	MS^2[491]: 315(100), 175(23) MS^3[491 → 315]: 267(29), 265(29), 236(100), 149(32)	II	G	–	+	–	–	J	[8,25]
37	52.31	505	3′-*O*-Methylciolanone glucuronide	MS^2[505]: 329(100), 175(8) MS^3[505 → 329]: 314(88), 313(26), 299(91), 296(22), 283(100), 238(64), 137(34)	II	G	–	+	–	–	J	[8,25]
40	54.78	425	5,7-Dihydroxy-2′,4′,5′-trimethoxyisoflavanone sulfate	MS^2[425]: 345(72), 249(100), 175(60), 131(38) MS^3[425 → 249]: 137(100)	II	S	–	+	+	–	J	[8,25]

Table 1 (*Continued*)

No.	Retention time, t_R (min)	$[M-H]^-$ (*m/z*)	$[M+H]^+$ (*m/z*)	Assigned identification	HPLC/ESI-MS^n *m/z* (% of relative abundance)	Type of metabolism[b]		Detected in[c]				Origin[d]	Ref.[e]
								P	B	U	F		
43	58.25	347		Formonoetin sulfate	MS^2[347]: 267(100) MS^3[347 → 267]: 252(100) MS^4[347 → 267 → 252]: 225(54), 224(100)	II	S	–		+	–	J	[8,25]
45	60.84	431		Pinocembrin glucuronide	MS^2[431]: 255(100), 175(26) MS^3[431 → 255]: 213(100)	II	G	+	+	–	–	J	[28]
46	60.99	255		Pinocembrin isomer	MS^2[255]: 213(100), 211(26), 164(12), 151(15) MS^3[255 → 213]: 185 (100)	I	X	–	+	–	–	J	[28]
50	65.64	379		Sativanone sulfate	MS^2[379]: 299(100) MS^3[379 → 299]: 284(86), 283(8), 269(59), 266(13), 162(16), 153(22), 136(15), 135(32)	II	S	+	–	–	–	J	[8,25]
Pinanes													
2	14.25	343		Mudanpioside F/G	MS^2[389]: 343(100) MS^3[389 → 343]: 180(100)	–	N/A[f]	–	–	+	+	C	[6]
3	16.70	495		Oxypaeoniflorin[a]	MS^2[541]: 495(100), 413(46), 381(74)	–	N/A[f]	–	–	–	+	C	
7	25.17	479		Paeoniflorin[a]	MS^2[525]: 479(10), 449(100), 327(7) MS^3[525 → 449]: 327(100), 309(16), 165(21) MS^4[525 → 449 → 327]: 165(100)	–	N/A[f]	+	+	+	+	C	
14	34.16	631		Galloylpaeoniflorin	MS^2[631]: 613(100), 601(9), 491(50), 463(7), 399(16), 313(7), 271(21), 211(8) MS^3[631 → 613]: 585(26), 491(100), 315(17), 313(17), 271(48)	–	N/A	–	–	–	+	C	[6]
Phthalides													
12	33.28		205	Hydroxybutylidenephthalide	MS^2[205]: 187(100), 149(18) MS^3[205 → 187]: 169(14), 159(100), 145(19), 141(10), 131(12)	I	O	–	+	–	–	X	[12]
15	34.43		227	Dihydroxyneocnidilide	MS^2[227]: 209(100), 191(9) MS^3[227 → 209]: 191(100), 163(40), 153(8), 145(9) MS^4[227 → 209 → 191]: 163(100), 149(98)	I	O	–	+	–	–	X	[13]
16	37.09		383	Hydroxyligustilide glucurnide	MS^2[383]: 364(6), 337(10), 329(6), 303(39), 291(26), 247(9), 207(100), 206(8), 195(10), 159(8) MS^3[383 → 207]: 189(100), 171(21), 119(33), 109(42)	II	G	–	+	–	–	X	[12]
21	40.74		515	Hydroxysenkyunolide A glutathione conjugate	MS[Full ms]515(47),385(100) MS^2[385]: 368(37), 367(62), 350(37), 282(13),207(100), 189(18), 162(83), 144(16), 116(7) MS^3[385 → 207]: 248(13), 229(43), 189(100), 165(10), 163(14), 161(34), 139(38), 133(47), 119(26) MS^4[385 → 207 → 189]: 105(100)	II	GSH	–	+	–	–	X	[12]
27	43.59		209	Hydroxysenkyunolide A	MS^2[209]: 191(70), 181(100), 167(7), 163(29), 149(71), 135(13)	I	O	–	+	–	–	X	[30]
32	47.10		497	Ligustilide glutathione conjugate	MS[Full ms] 497(5), 367(100) MS^2[367]: 349(32), 274(80), 246(24), 189(100), 179(48), 162(20) MS^3[367 → 189]: 187(14), 171(100), 143(22), 133(47)	II	GSH	–	+	–	–	X	[12]

[a] Compared with reference compounds.
[b] Type of metabolism: I, phase I metabolism; II, phase II metabolism; M, methylation; O, oxidation; H, hydrolysis; S, sulfation; G, glucuronidation; GSH, glutathion conjugate; X, others; N/A, prototype.
[c] Detect in: P, plasma; U, urine; F, feces; B, bile; +, detected in screening; –, not detected in screening.
[d] Origin: D, Radix Salviae Miltiorrhizae; C, Radix Paeoniae Rubra; H, Flos Carthami; J, Lignum Dalbergiae Odoriferae; X, Rhizoma Chuanxiong.
[e] Ref, literature referred to for structure assignment.
[f] Formylated (due to the formic acid in the mobile phase).

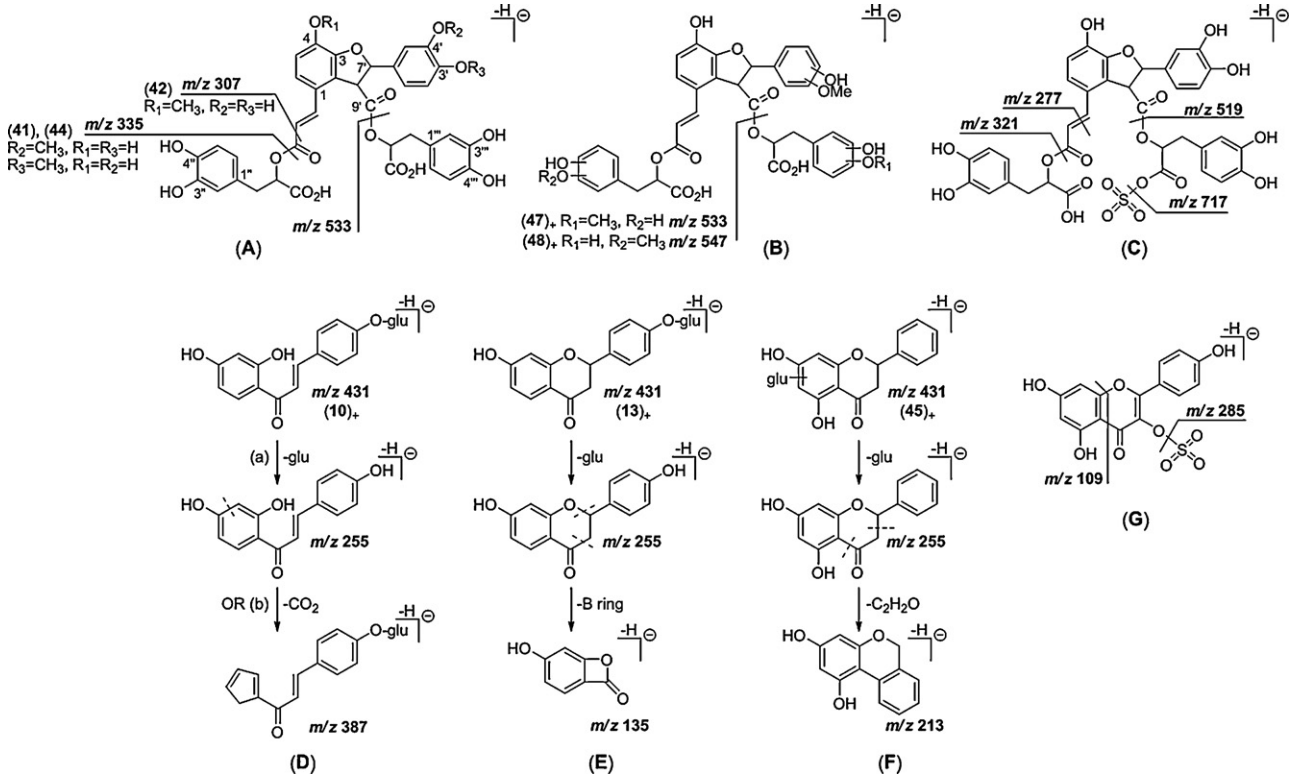

Fig. 2. Fragmentation patterns of assigned structures. (A) Prototypes **41**, **42**, and **44** (*m/z* 731); (B), metabolites **47** and **48** (*m/z* 745); (C), metabolite **33** (*m/z* 797); (D)–(F), metabolites **10**, **13**, and **45** (*m/z* 431); (G), metabolite **28** (*m/z* 365).

was apt to eliminate in MS fragmentation (Fig. 1B2–3). By comparing its MS^n spectra with a reference standard of salvianolic acid B (Fig. 1A2–4), peak **33** was identified as salvianolic acid B -*O*-sulfate (Fig. 2C). Peak **5** was assigned as benzoyl glycine, which could be attributed to various biotransformation of salvianolic B [27].

3.2.2. Flavonoids

For flavonoids and their glycosides, 2 prototypes and 20 metabolites were identified. Peak **4** was identified as hydroxysafflor yellow A by comparing with reference standard. Peak **25** was assigned as butin based on a previous report on the chemical analysis of GX II [9]. Peaks **8**, **9**, **10**, **13**, **19**, **30**, **36**, **37** and **45** were glucuronidated conjugates as their $[M-H]^-$ ions exhibited the characteristic neutral loss of glucuronic acid at 176 u [25], and produced $[A-H]^-$ (A = aglycone) ions in correspondence with their flavonoid skeletons (Fig. 2D–F). Peaks **18**, **23**, **28**, **40**, **43** and **50** were proposed as sulfate conjugates, because their $[M-H]^-$ ions showed neutral loss of 80 u [25] which complied with sulfur trioxide (SO_3) (Fig. 2G). By comparing the fragmentation pattern of compound **9** (Fig. 1D1–3) with reference standard kaempferol-3-*O*-β-rutinoside (**r3**) (Fig. 1C1–3), compound **9** was assigned to the same kaempferol skeleton, which was substituted by glucuronic acid.

All conjugations above shared similar-structured parent compounds that triggered $[A-H-15]^-$ and $[A-H-18]^-$ due to the loss of CH_3 and H_2O, respectively [8,28]. Their MS^3 and MS^4 spectra were compared with previous study [8] for the identification of aglycone skeletons. Notably, compared with constituents in GX II prescription, these aglycone skeletons were either prototypes or methylated/hydroxylated metabolites. Peak **11** (*m/z* 527), which displayed successive losses of 176 u and 80 u, produced $[A-H]^-$ at *m/z* 271. It was tentatively identified as butein [8], substituted by both glucuronic acid and sulfate. The fragment at *m/z* 151 in MS^4 was derived from RDA cleavage. Flavonoids exhibited extensive distribution in plasma, urine and feces, mainly in their metabolized form.

3.2.3. Pinanes

Compounds with pinane structures from GX II were monoterpenoid glycosides. Peaks **2**, **3**, and **7** yielded $[M+HCOO]^-$ ions at *m/z* 389, *m/z* 541, and *m/z* 525, while peak **14** exhibited $[M-H]^-$ at *m/z* 631. Their MS/MS spectra showed neutral losses of 30 u, 122 u, 162 u and 180 u, due to the eliminations of methoxyl, benzoic acid, glucosyl group and glucose. MS spectra of compound **7** were shown in Fig. 1E1–4. By comparing with previous report [9], peaks **2**, **3**, **7** and **14** were assigned as mudanpioside F/G, oxypaeoniflrin, paeoniflorin and galloylpaeoniflorin, respectively. Pinane metabolites were not detected due to their poor oral bioavailability [29].

3.2.4. Phthalides

Six phthalide metabolites were detected in MS positive mode, through which a glutathione (GSH) conjugation pathway was suggested. Peaks **12**, **15** and **27** all yielded $[M+H-18]^+$ or $[M+H-36]^+$ promptly after exhibiting $[M+H]^+$ ions at *m/z* 205, *m/z* 227 and *m/z* 209, indicating single or multiple hydroxyl groups. According to the previous reports, they were assigned as hydroxybutylidenephthalide, dihydroxyneocnidilide, and hydroxysenkyunolide A, respectively [12,13,30]. Due to their absence in GX II decoction [9], these hydroxylated derivates were proposed to be metabolites. Peak **16**, exhibiting $[M-H-176]^+$ at *m/z* 207, was identified as hydroxyligustilide glucuronide [12]. Peaks **21** (*m/z* 515) and **32** (*m/z* 497, Fig. 1G1–3) produced remarkable fragments following distinctive pathway of glutathione conjugate. Predominant fragment ions observed were $[M+H-130]^+$ and $[M+H-307]^+$, which was at *m/z* 385, 207 for compound **21**, and at *m/z* 367, 189 for compound **32**. The neutral losses of 130 u and 307 u suggested substitution of glutamate and glutathione, respectively. By comparing their mass

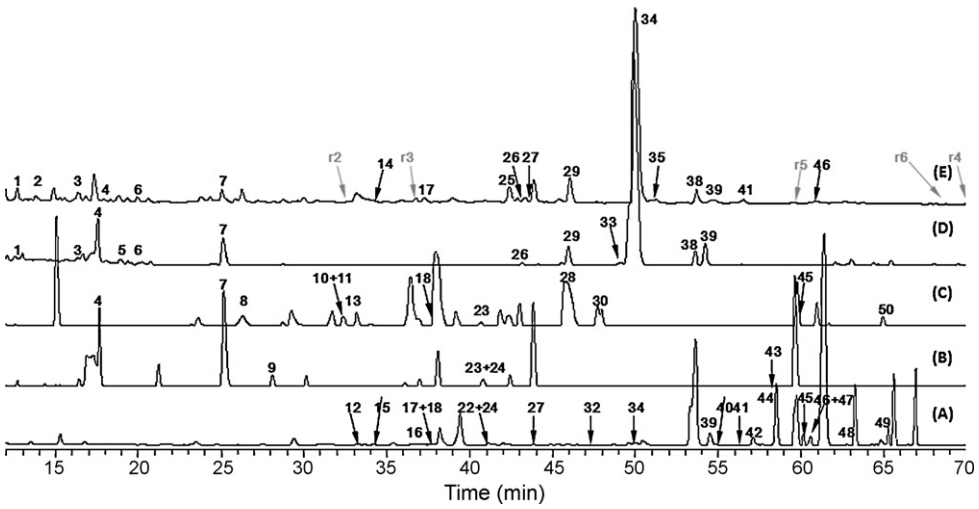

Fig. 3. Total ion current (TIC) metabolic fingerprints of biological samples after oral administration of GX II. (A) 0–12 h bile; (B) 0–12 h urine; (C) 30 min plasma; (D) 0–12 h feces; (E) GX II extract.

spectra with those of ligustilide (**r6**) (Fig. 1F1–3), peaks **21** and **32** were identified as glutathione conjugates of hydroxysenkyunolide A [12] and ligustilide, respectively.

3.3. Metabolic fingerprints and proposed metabolic pathways of major compounds

The total ion currents (TIC) of various biological samples were compared, as illustrated in Fig. 3 and Fig. 1S. To avoid the interference from endogenous components, background subtract was processed by Xcalibur™ 1.3 software. Biological samples from the control group were used as background signals.

Firstly, metabolites from GX II prescription were compared with metabolites from component herbs in same type of biological samples. The aim of these comparisons was to find the responsible component herb for each metabolite. Fig. 1S showed a comparison example of biliary metabolites. It was observed that all compounds with phenolic acid skeleton came from Radix Salviae Miltiorrhizae, in which they were reported as bioactive constituents [3]. In the same manner, all pinane glycosides were attributed to Radix Paeoniae Rubra, exhibiting poor oral bioavailability [29]. All phthalides were from Rhizoma Chuanxiong and they were detected only in the positive ionization mode. The flavonoids and their glucosides were from Lignum Dalbergiae Odoriferae and Flos Carthami (Table 1).

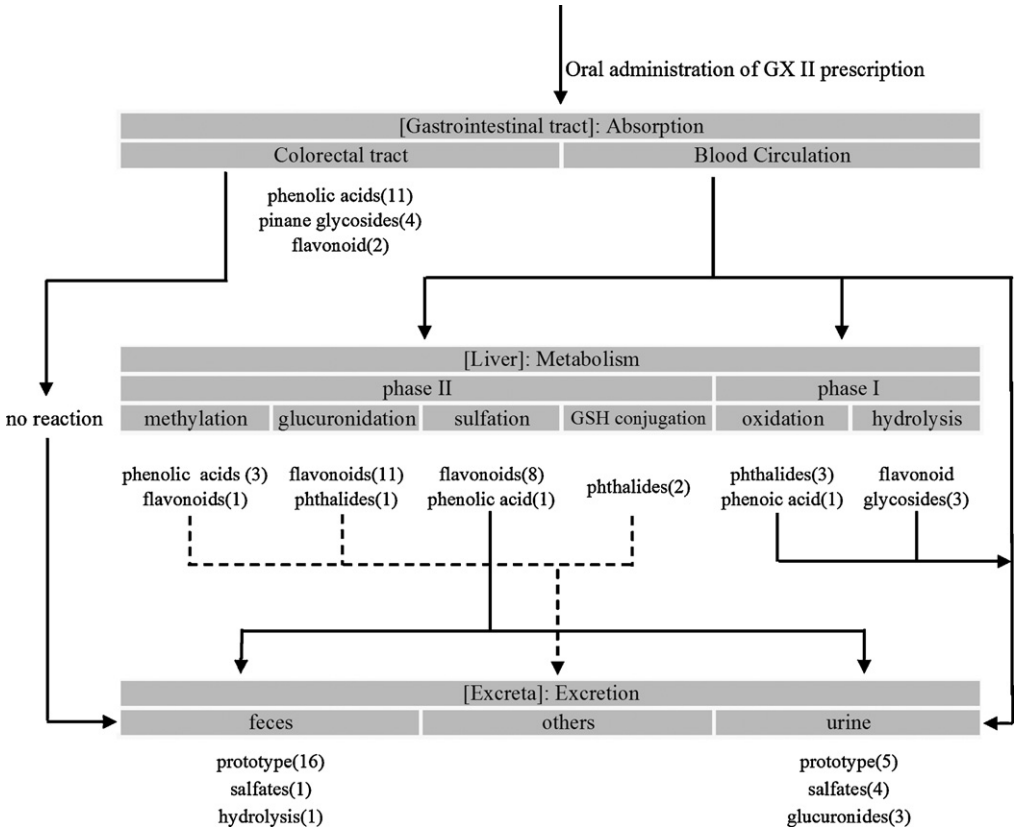

Fig. 4. Proposed metabolic pathways of GX II in rats after oral administration.

Secondly, GX II metabolic fingerprints (plasma, urine, feces, and bile) were aligned, and compared with the chemical fingerprint of GX II decoction (Fig. 3). The in vivo disposition pathways of the major compounds were proposed and illustrated in Fig. 4.

The 50 characterized phytochemicals in biological samples of GX II contained 17 prototypes and 33 biotransformed products. Prototypes suggested lower oral bioactivity, which might result from p*K*a or intestinal flora degradation [29]. On the contrary, the 33 metabolites were derived from constituents which could be more effectively absorbed. Among various metabolites detected in plasma, flavonoids were much more abundant than phenolic acids, pinanes, and phthalides. These results were in consistent with previous report [25].

Drug metabolism involved two types of enzyme-catalyzed reactions, phase I and phase II. Phase I reactions introduced a functional group into the parent molecule, including oxidation of phenolic acids, pinanes and hydrolysis of flavonoid glycosides. Phase II reactions conjugated endogenetic molecules with xenobiotic molecules to alter p*K*a. Sulfation and glucuronidation were most common for GX II, especially for flavonoids. Glutathione conjugation and methylation were mainly detected for phthalide and phenolic acids, respectively. Sulfation, glucuronidation and glutathione increased hydrophilicity and excretion, while methylation increased lipophilicity and reabsorption.

For the excretion of GX II, fecal metabolites were primarily hydrophobic prototypes, while urinary metabolites were phase II metabolites or hydrophilic prototypes. Phase II metabolites, especially sulfates, were rapidly excreted within 12 h. In contrast, no phase I metabolites were excreted 0–12 h after administration, suggesting that phase I reactions prolonged exposure time. Besides, the absence of certain metabolites in excretes may as well indicate their elimination and structural transformation.

4. Conclusion

The metabolic fingerprint of GuanXin II decoction, a complicated TCM prescription, was established using HPLC–DAD–ESI-MS^n. In total, 50 metabolites were identified from rat plasma, bile, urine, and feces samples following oral administration. In addition, metabolic pathways of major compounds were summarized to elucidate the GX II metabolic profile. This is the first metabolic study of GX II, which systematically demonstrated the metabolic fate of a multi-component and multi-target formula through LC/MS-based metabolic fingerprints.

Acknowledgements

This work was supported by Program for Changjiang Scholars and Innovation Team in University (no. 985-2-063-112) and the Cultivation Fund of the Key Scientific and Technical Innovation Project, Ministry of Education of China (no. 104218).

Appendix A. Supplementary data

Supplementary data associated with this article can be found, in the online version, at doi:10.1016/j.jpba.2010.10.017.

References

[1] G. Ye, Y.Z. Li, Y.Y. Li, H.Z. Guo, D.A. Guo, SPE-HPLC method for the determination and pharmacokinetic studies on paeoniflorin in rat serum after oral administration of traditional Chinese medicinal preparation Guan-Xin-Er-Hao decoction, J. Pharm. Biomed. Anal. 33 (2003) 521–527.
[2] X.G. Yang, B. Peng, G.H. Zhang, L.L. Wei, S.F. Nie, W.S. Pan, Studies of the pharmacokinetics of paeoniflorin in two Jing-Zhi-Guan-Xin formulations after oral administration to beagle dogs, J. Pharm. Biomed. Anal. 41 (2006) 320–324.
[3] A.H. Liu, H. Guo, M. Ye, Y.H. Lin, J.H. Sun, M. Xu, D.A. Guo, Detection, characterization and identification of phenolic acids in Danshen using high-performance liquid chromatography with diode array detection and electrospray ionization mass spectrometry, J. Chromatogr. A 1161 (2007) 170–182.
[4] S.L. Li, S.S.K. Chan, G. Lin, L. Ling, R. Yan, H.S. Chung, Y.K. Tam, Simultaneous analysis of seventeen chemical ingredients of *Ligusticum chuanxiong* by on-line high performance liquid chromatography-diode array detector-mass spectrometry, Planta Med. 69 (2003) 445–451.
[5] L. Kong, Z.Y. Yu, Y.M. Bao, X.Y. Su, H.F. Zou, X. Li, Screening and analysis of an antineoplastic compound in Rhizoma Chuanxiong by means of in vitro metabolism and HPLC–MS, Anal. Bioanal. Chem. 386 (2006) 264–274.
[6] S.L. Li, J.Z. Song, F.F.K. Choi, C.F. Qiao, Y. Zhou, Q.B. Han, H.X. Xu, Chemical profiling of Radix Paeoniae evaluated by ultra-performance liquid chromatography/photo-diode-array/quadrupole time-of-flight mass spectrometry, J. Pharm. Biomed. Anal. 49 (2009) 253–266.
[7] L. Fan, H.Y. Zhao, M. Xu, L. Zhou, H. Guo, J. Han, B.R. Wang, D.A. Guo, Qualitative evaluation and quantitative determination of 10 major active components in *Carthamus tinctorius* L. by high-performance liquid chromatography coupled with diode array detector, J. Chromatogr. A 1216 (2009) 2063–2070.
[8] R.X. Liu, M. Ye, H.Z. Guo, K.S. Bi, D.A. Guo, Liquid chromatography/electrospray ionization mass spectrometry for the characterization of twenty-three flavonoids in the extract of *Dalbergia odorifera*, Rapid Commun. Mass Spectrom. 19 (2005) 1557–1565.
[9] X. Qiao, J. Han, M. Xu, Z.C. Zhang, S.F. Sun, H.F. Li, B.R. Wang, M. Ye, D.A. Guo, Characterization of chemical constituents in Guan Xin II decoction by liquid chromatography coupled with electrospray ionization-mass spectrometry, Planta Med. 74 (2008) 1720–1729.
[10] X.C. Li, C. Yu, Y.L. Lu, Y.L. Gu, J. Lu, W. Xu, L.J. Xuan, Y.P. Wang, Pharmacokinetics, tissue distribution, metabolism, and excretion of depside salts from *Salvia miltiorrhiza* in rats, Drug Metab. Dispos. 35 (2007) 234–239.
[11] Z.Q. Liu, Z.H. Jiang, L. Liu, M. Hu, Mechanisms responsible for poor oral bioavailability of paeoniflorin: role of intestinal disposition and interactions with sinomenine, Pharm. Res. 23 (2006) 2768–2780.
[12] R. Yan, K.N. Ling, S.L. Li, Y.K. Tam, G. Lin, Pharmacokinetics and metabolism of ligustilide, a major bioactive component in Rhizoma Chuanxiong, in the rat, Drug Metab. Dispos. 36 (2008) 400–408.
[13] K. Sekiya, Y. Tezuka, K. Tanaka, J.K. Prasain, T. Namba, K. Katayama, T. Koizumi, M. Maeda, T. Kondo, S. Kadota, Distribution, metabolism and excretion of butylidenephthalide of *Ligustici chuanxiong* rhizoma in hairless mouse after dermal application, J. Ethnopharmacol. 71 (2000) 401–409.
[14] Y. Li, Z.Y. Zhang, J.L. Zhang, Determination of hydroxysafflor yellow A in rat plasma and tissues by high-performance liquid chromatography after oral administration of safflower extract or safflor yellow, Biomed. Chromatogr. 21 (2007) 326–334.
[15] J.L. Zhang, M. Cui, Y. He, H.L. Yu, D.A. Guo, Chemical fingerprint and metabolic fingerprint analysis of Danshen injection by HPLC–UV and HPLC–MS methods, J. Pharm. Biomed. Anal. 36 (2005) 1029–1035.
[16] Z. Wen, T.E. Dumas, S.J. Schrieber, R.L. Hawke, M.W. Fried, P.C. Smith, Pharmacokinetics and metabolic profile of free, conjugated, and total silymarin flavonolignans in human plasma after oral administration of milk thistle extract, Drug Metab. Dispos. 36 (2008) 65–72.
[17] M. Urpi-Sarda, M. Monagas, N. Khan, R. Llorach, R.M. Lamuela-Raventós, O. Jáuregui, R. Estruch, M. Izquierdo-Pulido, C. Andrés-Lacueva, Targeted metabolic profiling of phenolics in urine and plasma after regular consumption of cocoa by liquid chromatography-tandem mass spectrometry, J. Chromatogr. A 1216 (2009) 7258–7267.
[18] H. Tsutsui, T. Maeda, T. Toyo'oka, J.Z. Min, S. Inagaki, T. Higashi, Y. Kagawa, Practical analytical approach for the identification of biomarker candidates in prediabetic state based upon metabonomic study by ultraperformance liquid chromatography coupled to electrospray ionization time-of-flight mass spectrometry, J. Proteome Res. 9 (2010) 3912–3922.
[19] M. Coen, E. Holmes, J.C. Lindon, J.K. Nicholson, NMR-based metabolic profiling and metabonomic approaches to problems in molecular toxicology, Chem. Res. Toxicol. 21 (2008) 9–27.
[20] K.K. Pasikanti, P.C. Ho, E.C.Y. Chan, Gas chromatography/mass spectrometry in metabolic profiling of biological fluids, J. Chromatogr. B 871 (2008) 202–211.
[21] P. Wang, Y. Liang, N. Zhou, B. Chen, L. Yi, Y. Yu, Z. Yi, Screening and analysis of the multiple absorbed bioactive components and metabolites of Dangguibuxue decoction by the metabolic fingerprinting technique and liquid chromatography/diode-array detection mass spectrometry, Rapid Commun. Mass Spectrom. 21 (2007) 99–106.
[22] F. Xu, Y. Zhang, S. Xiao, X. Lu, D. Yang, X. Yang, C. Li, M. Shang, P. Tu, S. Cai, Absorption and metabolism of Astragali Radix decoction: in silico, in vitro, and a case study in vivo, Drug Metab. Dispos. 34 (2006) 913–924.
[23] H. Kong, M. Wang, K. Venema, A. Maathuis, R. van der Heijden, J. van der Greef, G. Xu, T. Hankemeier, Bioconversion of red ginseng saponins in the gastro-intestinal tract in vitro model studied by high-performance liquid chromatography-high resolution Fourier transform ion cyclotron resonance mass spectrometry, J. Chromatogr. A 1216 (2009) 2195–2203.
[24] H. Idborg, L. Zamani, P.-O. Edlund, I. Schuppe-Koistinen, S.P. Jacobsson, Metabolic fingerprinting of rat urine by LC/MS Part 2. Data pretreatment methods for handling of complex data, J. Chromatogr. B 828 (2005) 14–20.
[25] M. Holčapek, L. Kolářová, M. Nobilis, High-performance liquid chromatography–tandem mass spectrometry in the identification and determination of phase I and phase II drug metabolites, Anal. Bioanal. Chem. 391 (2008) 59–78.
[26] X.C. Li, C. Yu, L. Wang, Y.L. Lu, W.Y. Wang, L.J. Xuan, Y.P. Wang, Simultaneous determination of lithospermic acid B and its three metabolites by liquid

chromatography/tandem mass spectrometry, J. Pharm. Biomed. Anal. 43 (2007) 1864–1868.
[27] M. Xu, H. Guo, J. Han, S.F. Sun, A.H. Liu, B.R. Wang, X.C. Ma, P. Liu, X. Qiao, Z.C. Zhang, D.A. Guo, Structural characterization of metabolites of salvianolic acid B from *Salvia miltiorrhiza* in normal and antibiotic-treated rats by liquid chromatography–mass spectrometry, J. Chromatogr. B 858 (2007) 184–198.
[28] J. Guo, D. Liu, D. Nikolic, D. Zhu, J.M. Pezzuto, R.B. van Breemen, In vitro metabolism of isoliquiritigenin by human liver microsomes, Drug Metab. Dispos. 36 (2008) 461–468.
[29] S. Takeda, T. Isono, Y. Wakusi, Y. Matsuzaki, H. Sasaki, S. Amagaya, M. Maruno, In vivo assessment of extrahepatic metabolism of paeoniflorin in rats: relevance to intestinal floral metabolism, J. Pharm. Pharmacol. 49 (1997) 35–39.
[30] R. Yan, G. Lin, K.N. Ling, Y.K. Tam, Low oral bioavailability and pharmacokinetics of senkyunolide A, a major bioactive component in Rhizoma Chuanxiong, in the rat, Ther. Drug. Monit. 29 (2007) 49–56.